



Technological University Dublin
ARROW@TU Dublin

Articles

School of Chemical and Pharmaceutical
Sciences

2008

Improved High-Temperature Stability and Sun-Light-Driven Photocatalytic Activity of Sulfur-Doped Anatase TiO₂

Suresh Pillai

Technological University Dublin, suresh.pillai@tudublin.ie

Declan McCormack

Technological University Dublin, Declan.mccormack@tudublin.ie

Pradeepan Periyat


pradeepan.periyat@tudublin.ie

John Colreavy

Technological University Dublin, john.colreavy@tudublin.ie

Steve Hinder

Follow this and additional works at: <https://arrow.tudublin.ie/scschcpsart>
University of Surrey

 Part of the [Analytical Chemistry Commons](#), [Engineering Commons](#), [Inorganic Chemistry Commons](#), and the [Physical Chemistry Commons](#)

Recommended Citation

Pillai, S. et al. (2008) : Improved High-Temperature Stability and Sun-Light-Driven Photocatalytic Activity of Sulfur-Doped Anatase TiO₂. *Journal of Physical Chemistry C*, 112 (20), 2008, 44–7652. doi:10.1021/jp0774847

This Article is brought to you for free and open access by the School of Chemical and Pharmaceutical Sciences at ARROW@TU Dublin. It has been accepted for inclusion in Articles by an authorized administrator of ARROW@TU Dublin. For more information, please contact yvonne.desmond@tudublin.ie, arrow.admin@tudublin.ie, brian.widdis@tudublin.ie.



This work is licensed under a [Creative Commons Attribution-Noncommercial-Share Alike 3.0 License](#)



Improved High-Temperature Stability and Sun-Light-Driven Photocatalytic Activity of Sulfur-Doped Anatase TiO₂

Pradeepan Periyat,^{†,‡} Suresh C. Pillai,^{*,†} Declan E. McCormack,[‡] John Colreavy,[†] and Steven J. Hinder[§]

Centre for Research in Engineering Surface Technology (CREST), FOCAS Institute, Dublin Institute of Technology, Camden Row, Dublin 8, Ireland, School of Chemical and Pharmaceutical Sciences, Dublin Institute of Technology, Kevin Street, Dublin 8, Ireland, and The Surface Analysis Laboratory, School of Engineering, University of Surrey, Guildford, Surrey GU2 7XH, U.K.

Received: September 17, 2007; Revised Manuscript Received: February 29, 2008; In Final Form: March 5, 2008

Of the various forms of titania (anatase, rutile, and brookite), anatase is reported to be the best photocatalyst. The anatase-to-rutile transformation in pure synthetic titania usually occurs at a temperature range of 600–700 °C. High-temperature (≥ 800 °C) stable anatase titania photocatalyst is required for antibacterial applications in building materials. A simple methodology to extend the anatase phase stability by modifying the titanium isopropoxide precursor with sulfur modification using sulfuric acid is presented. Various TTIP/H₂SO₄ molar ratios such as 1:1, 1:2, 1:4, 1:8, and 1:16 were prepared, and these samples were characterized by XRD, DSC, Raman spectroscopy, XPS, and BET surface area analysis. Sulfur-modified samples showed extended anatase phase stability up to 900 °C, while the control sample prepared under similar conditions completely converted to rutile at 800 °C. Stoichiometric modification up to 1:4 TTIP/H₂SO₄ composition (TS4) was found to be most effective in extending the anatase-to-rutile phase transformation by 200 °C compared to that of the control sample and showed 100% anatase at 800 °C and 20% anatase at 900 °C. The TS4 composition calcined at various temperatures such as 700, 800, 850 and 900 °C showed significantly higher photocatalytic activity compared to the control sample. The TS4 composition calcined at 850 °C showed visible light (sunlight) photocatalytic activity, and it decolorized the rhodamine 6G dye within 35 min (rate constant, 0.069 min⁻¹), whereas the control sample prepared under identical conditions decolorized the dye only after 3.5 h (rate constant, 0.007 min⁻¹). It was also observed that the optimal size for the highest photocatalytically active anatase crystal is ~ 15 nm. XPS studies indicated that the retention of the anatase phase at high temperatures is due to the existence of small amounts of sulfur up to 900 °C.

1. Introduction

Nanocrystalline anatase titania has found various applications in areas such as photocatalysis, photovoltaics, nanochromic display devices, and self-cleaning coatings.^{1–8} A high-temperature stable anatase titania photocatalyst which is stable up to the curing temperature of ceramic substrates is particularly desirable for antibacterial material applications.^{2,9} Under normal condition, anatase titania is nonreversibly converted to rutile at a temperature range of 600–700 °C.⁸ Therefore, synthesis of a high-temperature (≤ 800 °C) stable anatase phase is one of the major challenges in the ceramic industries.⁹ Metal ion dopants have conventionally been used to extend the anatase phase stability at high temperatures.^{10–14} However, formation of various secondary impurity phases, such as metal titanates and/or metal oxides at high temperatures, is the major drawback of these methods.^{8,10} Secondary impurity phase formation will reduce the photocatalytic activity and phase stability of anatase titania.¹⁰ Chemical modification of the precursor by using organic materials is another method used to develop high-temperature stable anatase titania.² This eliminates the possibility of producing secondary impurity phases at high temperatures and

therefore improves the required properties of titania. Various chemical modifications have previously been reported by species such as urea, acetic acid, and trifluoroacetic acid.^{2,15,16} We have recently found that the incorporation of nitrogen using chemical modification of titanium isopropoxide by urea leads to the retention of 11% of the anatase phase at 900 °C.²

Colon et al. reported the enhanced photocatalytic activity of sulfated titania and sulfuric acid stabilized Cu-doped titania for phenol degradation.^{17,18} The material calcined at 700 °C was crystalline and contained 90% anatase, but it was completely transformed into rutile at 800 °C. Correlation between oxoanion (SO₄²⁻, NO₃⁻, and PO₄³⁻) stability during calcination and photocatalytic behavior of TiO₂ was also reported.¹⁹ These acid treatments led to an excess of adsorbed protons (Brønsted acid sites) incorporated onto the TiO₂ surface. Sulfur modification in TiO₂ using hydrothermal treatments were also reported.^{20,21} Ho et al. investigated the antibacterial effect of S-doped titania prepared using thiourea, and this study revealed that S-doped titania was effective in killing *Micrococcus lylae*, a gram positive bacterium.^{20,21} Recent literature reports indicate that sulfur could either add to the TiO₂ matrix as a cation or an anion depending upon the sulfur source employed.^{22,23} Umabayashi et al. reported that sulfur is doped as an anion in titania.²² This anion doping shifts the absorption spectrum of titania to a lower energy and effectively leads to visible light activity. Ohno et al. found out that S⁴⁺ substitutes some of the lattice Ti⁴⁺, leading to visible light activity.²³ Recently, visible light photoca-

* To whom correspondence should be addressed. E-mail: suresh.pillai@dit.ie.

[†] FOCAS Institute, Dublin Institute of Technology, Dublin Institute of Technology.

[‡] School of Chemical and Pharmaceutical Sciences.

[§] University of Surrey.

talysis of titania doped with sulfur or nitrogen has been studied and reviewed by several researchers.^{24–26}

A comparative study of two different Cu precursors, CuCl₂ and CuSO₄, for anatase stabilization was reported by Bokhimi et al., and they suggested that 10 wt % CuSO₄ addition was effective in retaining 98% anatase at 800 °C.²⁷ The stabilization explained in these previous studies may not only be due to the sulfate ions but is more likely due to the combined effect of Cu²⁺ and SO₄²⁻.^{17,18,27} It should also be noted that upon 10 wt % addition of CuSO₄, copper segregated as bonattite (CuSO₄·3H₂O) after annealing the sample at 400 °C or a lower temperature and as antierite (Cu₃SO₄(OH)₄) after annealing the sample at 800 °C.²⁷

Although there are a few reports available in the literature on the pretreatment of titania using various inorganic acids such as sulfuric acid, nitric acid, and phosphoric acid to improve photocatalytic activity^{17,18,28} (using N, S, or P incorporation), there have been no systematic studies reported on the development of a high-temperature stable anatase titania photocatalyst using sulfur modification. Here, we report a simple systematic study of the preparation of high-temperature stable anatase titania photocatalyst through modification of the precursor titanium isopropoxide with various mole ratios of sulfuric acid (1:1, 1:2, 1:4, 1:8, and 1:16 TTIP/H₂SO₄). The effect of sulfur modification was studied by using various characterization techniques such as XRD, Raman spectroscopy, XPS, DSC, and BET surface area analysis. This study has further investigated the extent to which sulfur modification can improve the anatase phase stability. It also aims to identify how the chemical modification improves the photocatalytic activity of titania by incorporating sulfur in a titania matrix. The novelty of the current work is the development of a high-temperature stable photocatalytically active anatase phase stable up to 900 °C using S modification.

2. Experimental Section

2.1. Procedure. The procedure used in this study was straightforward. The reagents used were titanium isopropoxide (Aldrich 97%) and sulfuric acid (Aldrich 95–97%). All reagents were used as supplied, and no further purification was carried out. In a typical experiment, 1:4 TTIP/H₂SO₄ (TS4) precursor solution and 29.7 mL of titanium isopropoxide (Ti(OPr)₄) waereplaced in a beaker. To the above solution, 38.8 mL of concentrated H₂SO₄ (95–97%) dissolved in 180 mL of water was added. The solution was then stirred for 20 min and aged for 2 h at room temperature. The term aging indicates the time given for the completion of a reaction. In a sol–gel synthesis, this results in substantial structural reorganization of the gel network, which may or may not lead to the change in structure and properties of the materials prepared. It was then dried at 350 °C for 6 h. The dried powder was calcined at various temperatures (600, 700, 800, 850, and 900 °C) at a heating rate of 5 °C per minute and held at these temperatures for 2 h.

A similar procedure was adopted to synthesize 1:1, 1:2, 1:8, and 1:16 samples. Samples are named as TS1, TS2, TS8, and TS16, respectively. In all cases, the molar ratio of TTIP/H₂SO₄/H₂O is 1/*x*/100, where *x* corresponds to the 1, 2, 4, 8, or 16. A control sample without any sulfuric acid was also prepared to compare the results.

XRD patterns of the calcined gels were obtained with a Siemens D 500 X-ray diffractometer in the range of 2θ = 20–70° using Cu Kα radiation. The amount of rutile in the sample was estimated using the Spurr equation (eq 1).

$$F_R = \left[\frac{1}{1 + 0.8(I_A(101)/I_R(110))} \right] 100 \quad (1)$$

where, F_R is the mass fraction of rutile in the sample and $I_A(101)$ and $I_R(110)$ are the integrated main peak intensities of anatase and rutile, respectively. The crystal size of the control and TS4 sample was calculated by using the Scherrer equation (eq 2).

$$\varphi = \frac{0.9\lambda}{\beta \cos \theta} \quad (2)$$

where φ = crystallite size, λ = X-ray wavelength, θ = Bragg angle, and β = full width at half-maximum.

BET (Brunauer, Emmett, and Teller) surface area measurements and pore size analysis were carried out by nitrogen adsorption using a Quantachrome Nova 4200 surface area analyzer. The measurements were carried out at liquid nitrogen temperature after degassing the powder samples for 3 h at 300 °C.

Differential scanning calorimetry (DSC) analysis was carried out using a Rheometric Scientific DSC QC. A small amount (3 mg) of the dried precursor sample was heated from room temperature (25 °C) to 650 °C at a constant heating rate of 10 °C/min.

X-ray photoelectron spectroscopy (XPS) analyses were performed using a Thermo VG Scientific Sigma Probe spectrometer. The instrument employs a monochromated Al Kα X-ray source ($h\nu = 1486.6$ eV), which was used at 140 W. The area of analysis was approximately 500 μm in diameter for the samples analyzed. For survey spectra, a pass energy of 100 eV and a 0.4 eV step size were employed. For C 1s and Ti 2p high-resolution spectra, a pass energy of 20 eV and a 0.1 eV step size were used. For O 1s high-resolution spectra, a pass energy of 20 eV and a 0.2 eV step size were used. For S 2p high-resolution spectra, a pass energy of 50 eV and a step size of 0.2 eV were employed. Charge compensation was achieved using a low-energy electron flood gun. Quantitative surface chemical analyses were calculated from the high resolution core level spectra, following the removal of a nonlinear Shirley background.

2.2. Photocatalytic Study. In a typical experiment, 0.06 g of TS4 sample calcined at 850 °C was added to an aqueous solution of rhodamine 6G solution (50 mL, 5×10^{-6} M), and this suspension was irradiated in a Q-Sun Xenon solar simulator chamber (Intensity max., 0.68 W/m² at λ max. of 340 nm) with continuous and uniform stirring. The degradation of rhodamine dye was monitored by taking 4 mL aliquots at different intervals of time. These aliquots were centrifuged, and absorption spectra of the samples were recorded using as UV/vis spectrophotometer. Similar experiments were carried out for the control sample calcined at 850 °C. The sunlight-driven photocatalytic activity of the TS4 and control titania calcined at 850 °C was determined by carrying out the reaction under Dublin sunlight (October 27, 2007). The intensity of the sunlight was determined by a Solar Light Co. broad-band radiometer PMA 2107 (Philadelphia), which gave approximately 12.0 W/m². The rate of degradation was assumed to obey pseudo-first-order kinetics, and hence, the rate constant for degradation, *k*, was obtained from the first-order plot (eq 3).

$$\ln\left(\frac{A_0}{A}\right) = kt \quad (3)$$

where A_0 is the initial absorbance, A is the absorbance after a time (*t*), and *k* is the pseudo-first-order rate constant.

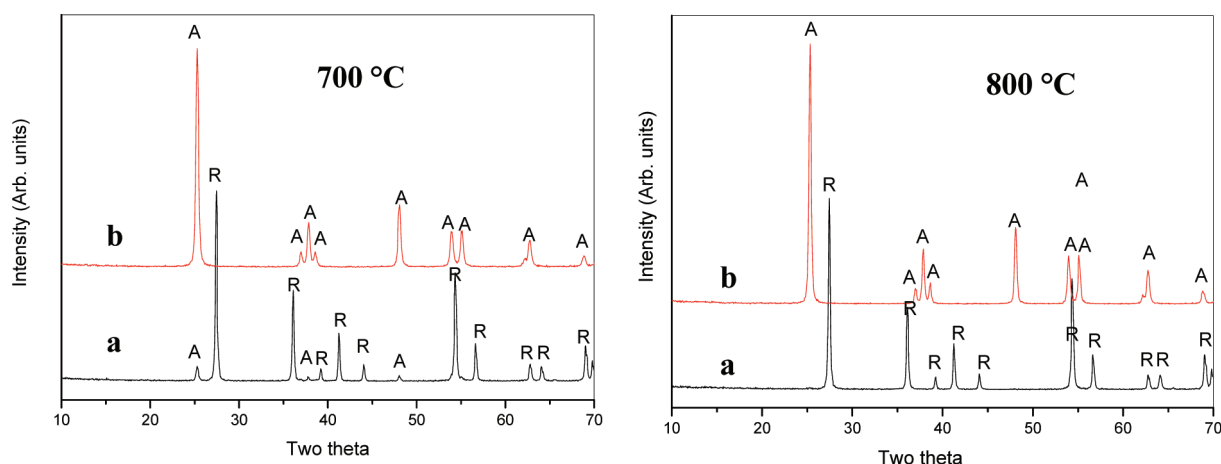


Figure 1. XRD spectra of calcined sample at 700 and 800 °C; (a) control, (b) TS4.

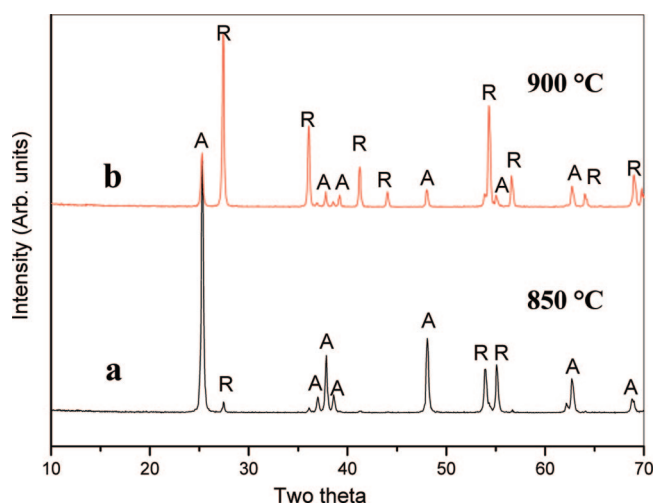


Figure 2. XRD spectra of TS4 sample calcined at (a) 850 and (b) 900 °C.

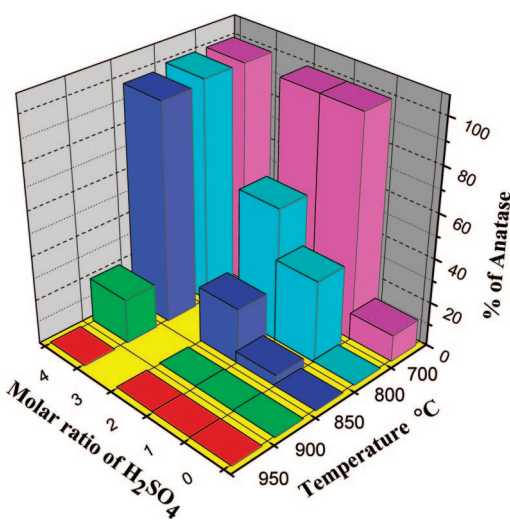


Figure 3. Anatase content in the control and various sulfur-modified samples (from XRD data) at different temperatures (error = ±5%).

192

3. Results

3.1. XRD Analysis. The anatase-to-rutile transformation of the calcined samples was studied by the powder X-ray diffraction (XRD) technique. The XRD patterns of the samples calcined at 700, 800, 850, and 900 °C are shown in Figures 1 and 2. The weight fraction of the anatase retained in the sample after various calcination temperatures was calculated by comparing the XRD-integrated intensities of the (101) reflection of anatase and the (110) reflection of rutile. It was found that 100% anatase TiO₂ was observed at the temperature of 800 °C for the sample prepared with or above TS4 composition. In comparison, it was found that even at 700 °C, the control sample showed 82% rutile, while in the case of the samples prepared with lower mole ratios of H₂SO₄ (TS1 and TS2), the anatase-to-rutile transformation commenced above 700 °C, and complete transformation to rutile occurred only at 900 °C (Figure 3). There is no notable influence on the anatase-to-rutile transformation temperature above TS4 modification. The TS8 and TS16 samples show similar phase distribution behavior up to 800 °C and were found to be slightly less effective in retaining the anatase phase at 900 °C compared to the TS4 sample. The optimum level of modification was found in the TS4 sample. The control sample was fully converted to rutile at 800 °C (Figure 1), while the TS4 sample retained 100% anatase at 800 °C, 98% anatase at 850 °C, and 20% anatase even at 900 °C (Figure 2 and 3).

3.2. Raman Studies. Raman spectroscopy was applied as an additional characterization tool to confirm the phase stability of titania at high temperatures. According to factor group analysis, the anatase phase consists of five Raman-active modes, while the rutile phase consists of four²⁹ (i.e., anatase: 144, 197, 395, 513, and 639 cm⁻¹; rutile: 143, 233, 447, and 610 cm⁻¹). Figure 4 indicates the Raman spectra of the control and TS4-modified sample calcined at 800 °C. All of the peaks present in the control sample were due to the rutile phase, and in the TS4 sample, all of the peaks were due to the anatase phase. The TS4 sample calcined at 900 °C (Figure 5) showed three anatase peaks which correspond to the amount of anatase phase present in the 900 °C sample. These results indicated that Raman spectroscopy studies were consistent with the XRD results.

3.3. XPS Analysis. XPS measurements were carried out to investigate the incorporation of sulfur in the titania matrix. It was previously reported that a sulfur-containing material shows a binding energy value of around 170 eV.¹⁸ The high-resolution XPS spectra of the S_{2p} region of the TS4 sample calcined at different temperatures, 700, 800, and 900 °C, are displayed in Figure 6. The presence of sulfur, carbon, oxygen, and titania in the samples was confirmed by XPS analysis. The presence of sulfur was confirmed by a peak at 168.4 eV (Figure 6). A previous literature report indicated that the peak at 168.4 eV is due to the presence of the S⁶⁺ cation.^{21,23b} In all S-modified samples, a peak at 168.4 eV was visible. In Figure 6a, the TS4

218
219
220
221
222
223
224
225
226
227
228
229
230
231
232
233
234
235
236
237
238
239
240
241
242
243

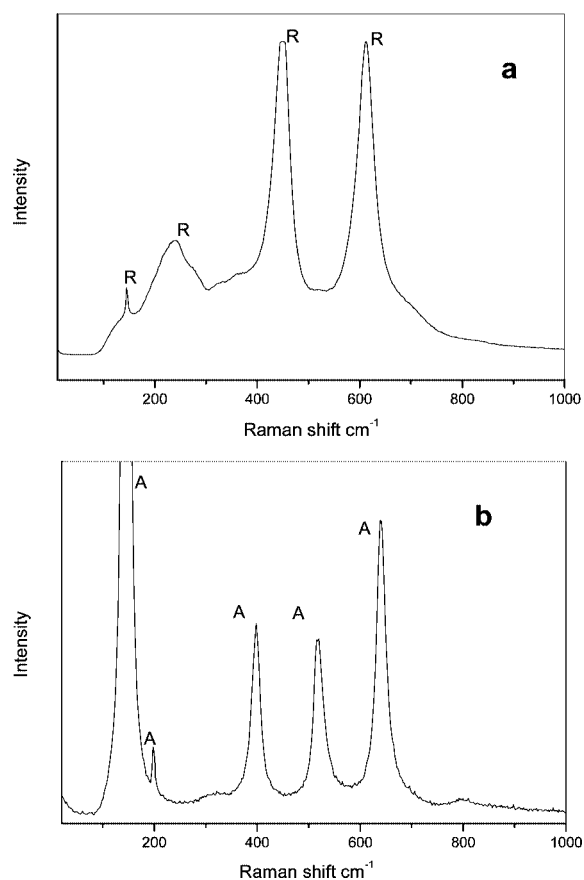


Figure 4. Raman spectra of the samples at 800 °C; (a) control, (b) TS4.

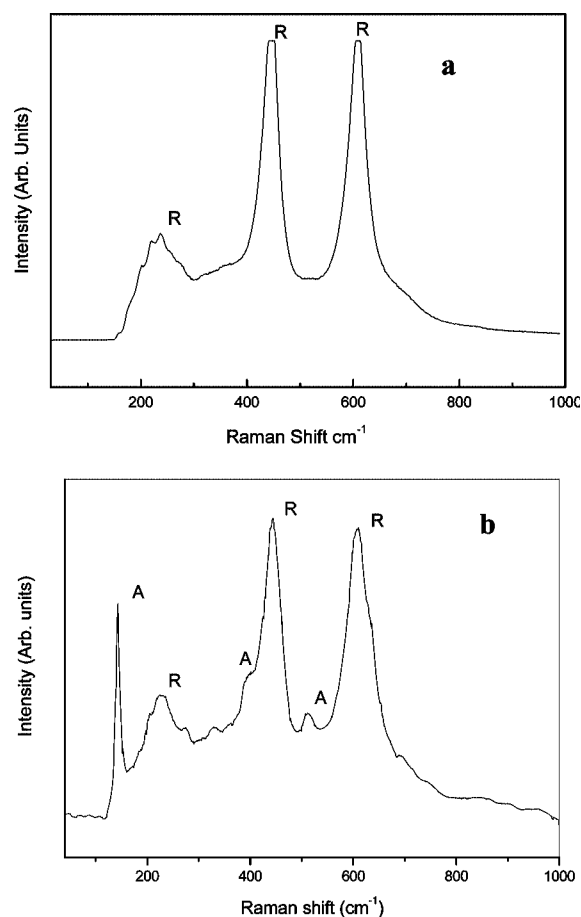


Figure 5. Raman spectra of the samples at 900 °C; (a) control, (b) TS4.

244 sample calcined at 700 °C shows a sharp peak at 168.4 eV, but
 245 at higher temperatures of 800 and 900 °C (Figure 6b and c),
 246 the peak becomes broad. This peak broadening observed in the
 247 high-binding energy side of the S peak (168.4 eV) can be
 248 attributed to two components, $S_{2p_{3/2}}$ and $S_{2p_{1/2}}$. These peaks
 249 are only ~ 1.1 eV apart and thus cannot be resolved from
 250 one another. Typically, the $S_{2p_{3/2}}$ peak at lower binding energy
 251 is about twice the intensity or area of the higher binding energy
 252 $S_{2p_{1/2}}$ peak. The XPS spectra of TS4 samples at 800 and 900
 253 °C (Figure 6b and c) show a small amount of peak splitting,
 254 which indicates that at higher temperature, there may be some
 255 amount of S^{4+} cation also present.^{23b} If the S concentration was
 256 higher, S^{6+} and S^{4+} peaks could be clearly resolved. However,
 257 as the sulfur amount present in the samples is less than 2 atom
 258 %, peak resolution is difficult. Table 1 shows that the presence
 259 of sulfur gradually reduces as the calcination temperature
 260 increases.

261 **3.4. BET Surface Area Analysis.** The BET surface area of
 262 the TS4 and control titania samples calcined at 700, 800, and
 263 900 °C are listed in Table 1. The TS4 sample calcined at 700
 264 °C showed a type-IV isotherm (Figure 7). The results indicated
 265 that the surface area of the samples was strongly dependent on
 266 the thermal treatment. The surface area of the TS4 sample
 267 decreased from 28 to 6 m^2/g as the calcination temperature
 268 increased from 700 to 900 °C. BET analysis of the TS4 sample
 269 calcined at higher temperatures showed a larger surface area
 270 (18 m^2/g at 800 °C and 6 m^2/g at 900 °C) compared to that of
 271 the control sample calcined at the same temperature (6.4 m^2/g
 272 at 800 °C and 0.96 m^2/g value at 900 °C). Therefore, the sulfur
 273 modification was found to increase the surface area of titania
 274 significantly.

275 **3.5. Photocatalytic Study.** In an attempt to assess the
 276 performance of the high-temperature stable anatase titania, the
 277 photocatalytic activity of the TS4 sample calcined at 850 °C
 278 and a similar control sample (Figure 8) was analyzed via a
 279 rhodamine 6G degradation. The control sample degraded the
 280 dye within 80 min, whereas the S-modified sample completely
 281 degraded the dye within 12 min. The control and the TS4 sample
 282 calcined at 700, 800, and 900 °C were also subjected to
 283 photocatalytic study (Supporting Information 1). The TS4
 284 sample calcined at 800 °C degraded the rhodamine dye within
 285 15 min, whereas the control (800 °C) required 40 min. This
 286 enhanced efficiency of the S-modified titania photocatalyst is
 287 reflected in kinetic analysis of the results (Supporting Informa-
 288 tion 1 and 2). The rhodamine degradation follows pseudo-first-
 289 order kinetics. First-order degradation rate constants, obtained
 290 by plotting the natural logarithm of the absorbance against
 291 irradiation time for the control and TS4 sample were calculated.
 292 The rate constant values recorded for the TS4 samples calcined
 293 at various temperatures were consistently and significantly
 294 superior to those recorded for the control samples under identical
 295 conditions (Supporting Information 1 and 2). Dark studies,
 296 where the above experiments were repeated in the absence of
 297 light, showed that there were no adsorption effects. A sample
 298 left for 24 h showed little change in absorbance of the rhodamine
 299 dye. The visible light (sunlight) activity of the S-doped materials
 300 has been examined. The results of sunlight photocatalytic
 301 activity are shown in Figure 9. The TS4 composition calcined
 302 at 850 °C decolorized the rhodamine 6G dye within 35 min
 303 (rate constant, 0.069 min^{-1}), whereas the control sample
 304 prepared under identical conditions decolorized the dye after

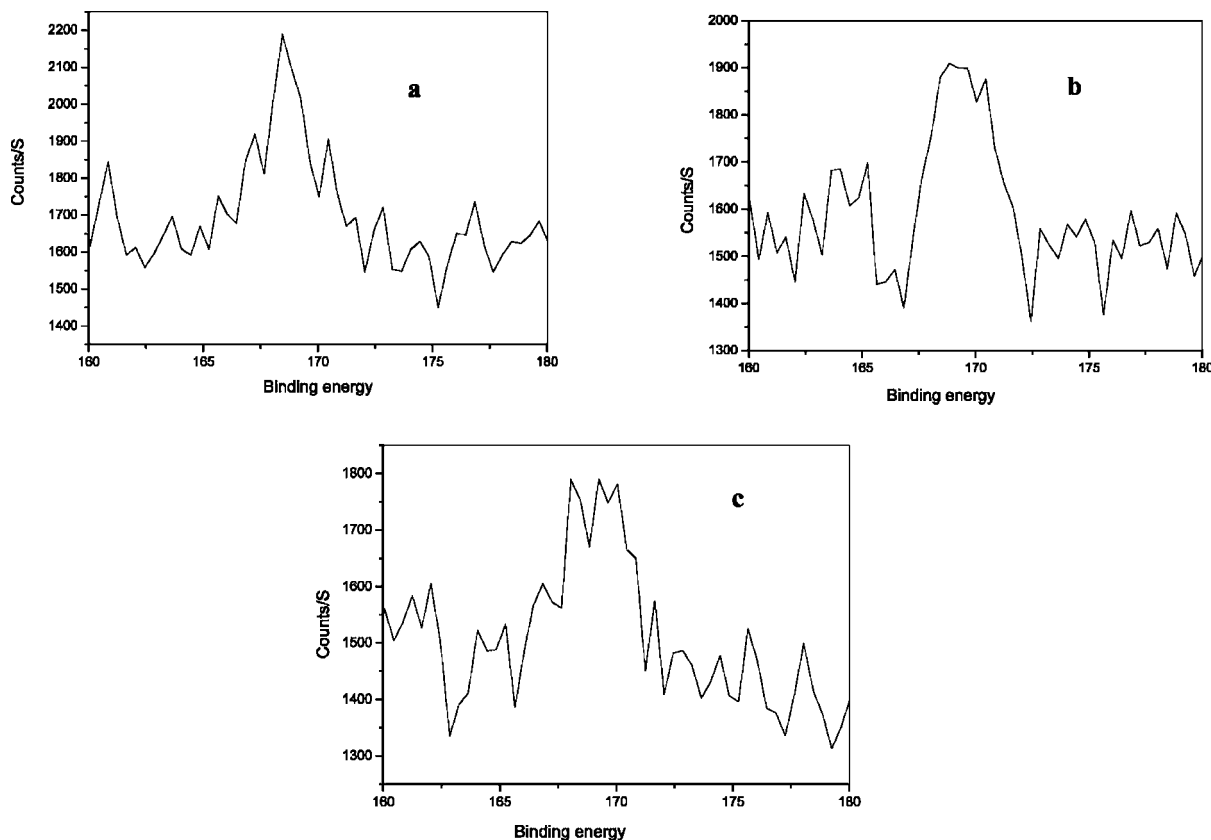


Figure 6. XPS spectra of TS4 samples calcined at (a) 700, (b) 800, and (c) 900 °C.

TABLE 1: Surface Area of the TS4 and Control Titania at Different Temperatures

sample	BET surface area (m ² /g) (±2.5%)	pore volume (cc/g)	pore diameter (nm)	sulfur content (atom %) by XPS (±5%)
TS4 800 °C	18.7	0.22	2.8	0.99
TS4 700 °C	28.1	0.37	44.1	1.24
TS4 900 °C	6.1	0.04	1.0	0.84
control 700 °C	25.6	0.16	14.2	0
control 800 °C	6.4	0.06	1.5	0
control 900 °C	1.0	0.00	1.0	0

4. Discussion

4.1. Anatase Phase Stability. Titanium isopropoxide reacts with water, and an aquo complex (Ti-OH₂)⁴⁺ is initially formed, which decomposed immediately to produce titanium hydroxo (Ti-OH)³⁺/oxo (Ti=O)²⁺ complex precipitates.³³ In order to avoid this faster hydrolysis (formation of the Ti-O bond) and condensation (removal of water or alcohol after the formation of the Ti-O bond), chemical additives (complexing molecules) are added to moderate the rate of the reaction.³⁴ This usually leads to the formation of a transparent sol instead of precipitating oxo/hydroxo complexes.^{33,35,36} The hydrolysis and condensation of titanium isopropoxide can be effectively controlled at a low pH.^{37,38} During the hydrolysis in the presence of an acid, the OR groups attached to the metal are protonated

3.5 h (rate constant, 0.007 min⁻¹). The rate constant values show that sulfur-doped titania has 10-fold greater photocatalytic activity compared to that of the control sample.

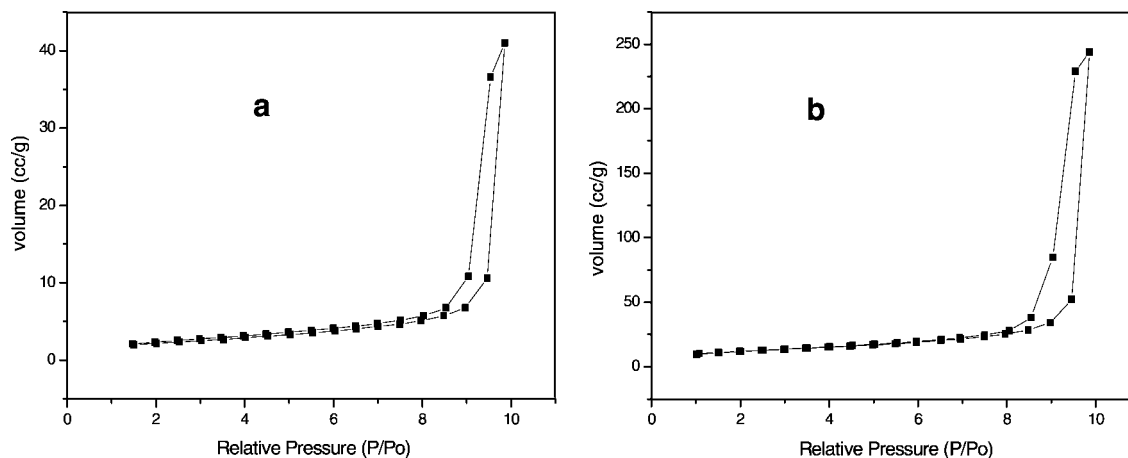


Figure 7. Type-IV isotherm of the sample calcined at 700 °C; (a) control, (b) TS4.

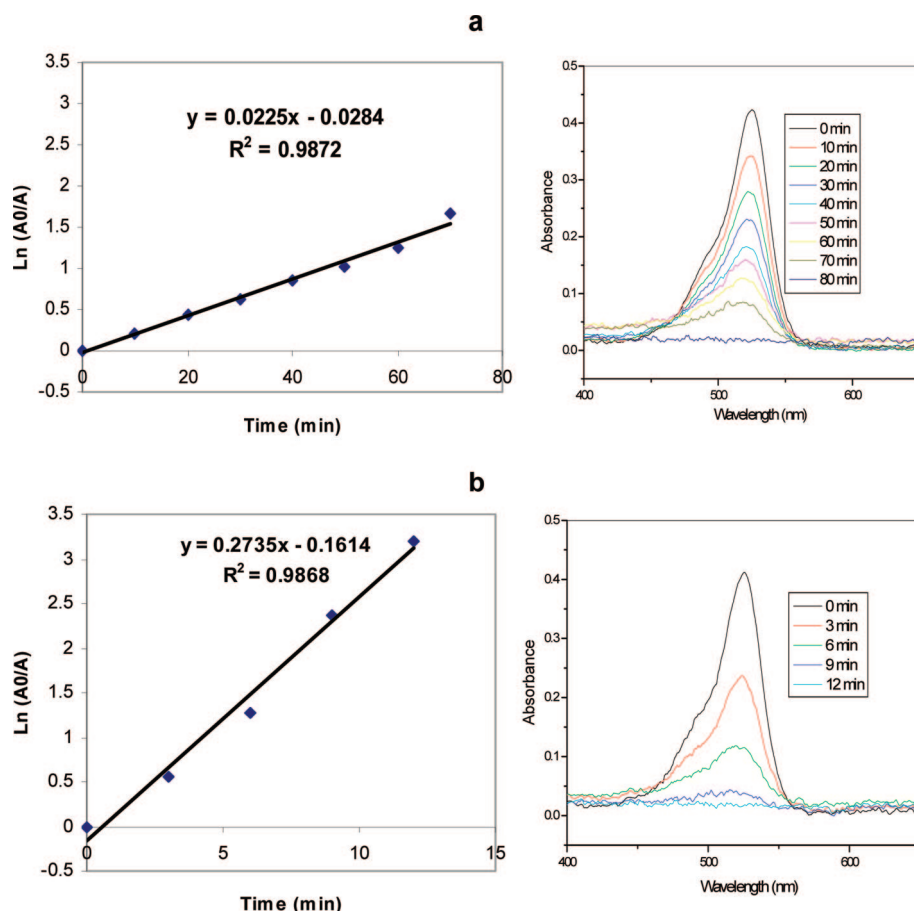
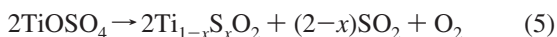
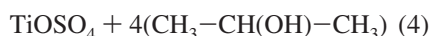


Figure 8. Kinetic study and absorption spectra of rhodamine dye degradation using (a) the control and (b) TS4 samples calcined at 850 °C under UV light. A_0 is the initial absorbance, and A is the absorbance after a time for the rhodamine dye degradation (error = $\pm 10\%$).

322 first by the H_3O^+ , which causes the OR group to reduce its
 323 electronegativity (its charge becomes more positive).^{37,38} The
 324 metal ion, which is already positively charged due to the
 325 electropositive nature, begins to repel the protonated OR. This
 326 repulsion between protonated species will decrease their interaction,
 327 which causes a rate of decrease in the condensation; hence,
 328 the rate of hydrolysis also decreases. In the present study,
 329 sulfuric acid was used as a chemical modifier; titanium
 330 isopropoxide reacted exothermally with sulfuric acid to form
 331 titanyl oxysulfate and thus decomposed at higher temperature
 332 to produce sulfur-doped titania, as indicated by eqs 4 and 5.



333
 334
 335
 336 The titanyl oxysulfate is stable up to a temperature of 600 °C,
 337 as indicated by the XRD (JCPDS file no. 81-1566) (Figure 10).
 338 DSC analysis of the sulfur-modified sample (TS4 sample)
 339 showed an endothermic peak at 620 °C (Figure 11) due to the
 340 decomposition of TiOSO_4 (eq 5). This is consistent with the
 341 XRD pattern at 700 °C (Figure 1), where the TS4 sample
 342 showed pure anatase phase only. This shows that above 600
 343 °C, TiOSO_4 began to decompose and formed the sulfur-doped
 344 anatase phase. The TiOSO_4 , which is stable up to 600 °C,
 345 indicated by the XRD and DSC results (Figures 10 and 11),
 346 has a basic structure (Scheme 1a) consisting of connected
 347 $[\text{TiO}_6]^{2-}$ octahedra and $[\text{SO}_4]^{2-}$ tetrahedra.³⁹ Upon further heat
 348 treatment of the TS4 sample above 600 °C, the decomposition
 349 of TiOSO_4 occurs (eq 5) to form the edge-shared anatase titania,

as shown in Scheme 1b. The final conversion to the thermo-
 350 dynamically stable rutile phase occurs at higher temperatures
 351 (900 °C), as illustrated in Scheme 1c. It has been reported that
 352 sulfur doping is difficult to achieve in titania due to the larger
 353 formation energy needed to substitute the oxygen by sulfur to
 354 form $\text{TiO}_{2-x}\text{S}_x$.^{40,41} Therefore, it is important to note that the
 355 TS4 sample contained 1.24, 0.99, and 0.84 atom % sulfur at
 356 700, 800, and 900 °C, respectively (Table 1). Thus sulfur doping
 357 was easily achieved by the decomposition of TiOSO_4 formed
 358 by the reaction between titanium isopropoxide and sulfuric acid
 359 (eq 5).
 360

Anatase (tetragonal, $a = b = 3.78 \text{ \AA}$; $c = 9.50 \text{ \AA}$) and rutile
 361 (tetragonal, $a = b = 4.58 \text{ \AA}$; $c = 2.95 \text{ \AA}$) are the two main
 362 crystalline forms of titania. It can also exist in brookite form
 363 (rhombohedral, $a = 5.43 \text{ \AA}$; $b = 9.16 \text{ \AA}$; $c = 5.13 \text{ \AA}$), although
 364 this particular phase did not occur at any stage of this study.
 365 Even though anatase and rutile exist in a tetragonal structure,
 366 experimental evidence indicates that anatase is more stable
 367 kinetically than rutile at room temperature and atmospheric
 368 pressure.^{2,37} Rutile is reported to be more stable thermodynamically
 369 than anatase at normal temperature.^{37,42} The thermodynamic
 370 phase stability calculation by Zhang and Banfield shows
 371 anatase titania transforms to rutile only after growing to a
 372 crystallite size of $\sim 14 \text{ nm}$.⁴²⁻⁴⁴ Below this critical size of ~ 14
 373 nm, the anatase phase is more stable. The crystallite sizes
 374 calculated by using the Scherrer equation (eq 3) for the TS4
 375 sample and control sample are shown in the Table 2. Here, in
 376 the case of the control titania mentioned above, the critical size
 377 is already exceeded at 700 °C (17.7 nm) itself, whereas the TS4
 378 sample reached this limit (15.7 nm) only after the calcination
 379

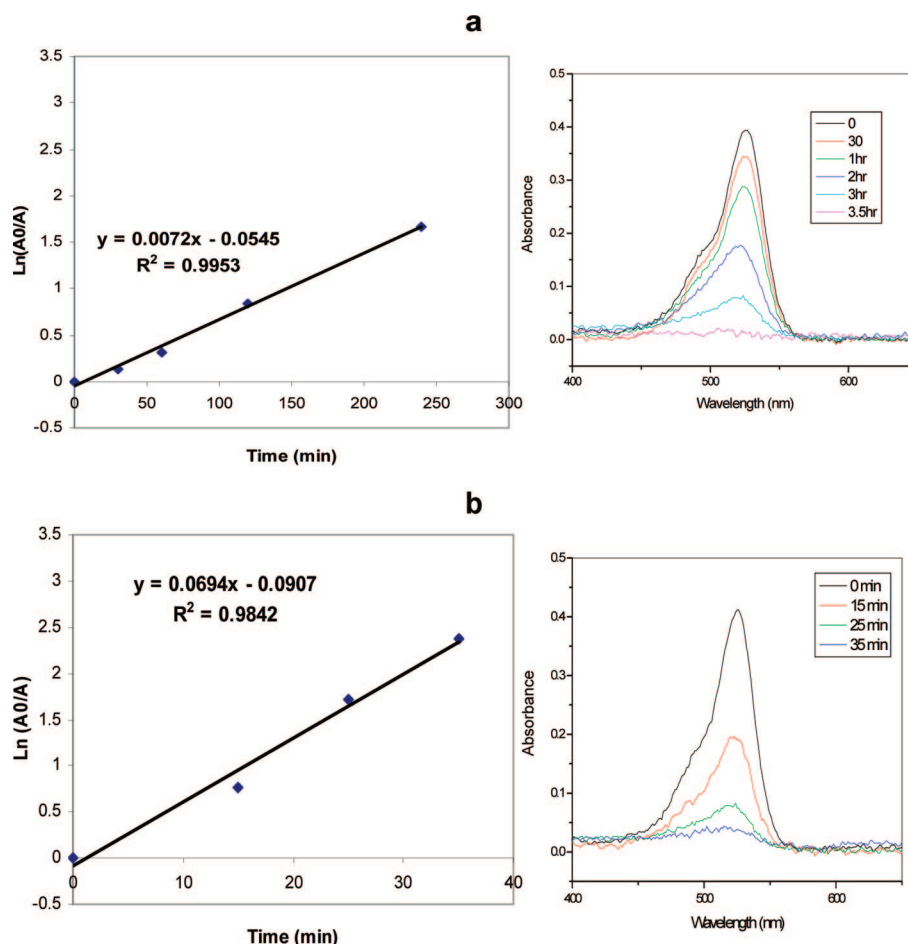


Figure 9. Kinetic study and absorption spectra of rhodamine dye degradation using (a) the control and (b) TS4 samples calcined at 850 °C under sunlight. A₀ is the initial absorbance, and A is the absorbance after a time for the rhodamine dye degradation (error = ±10%).

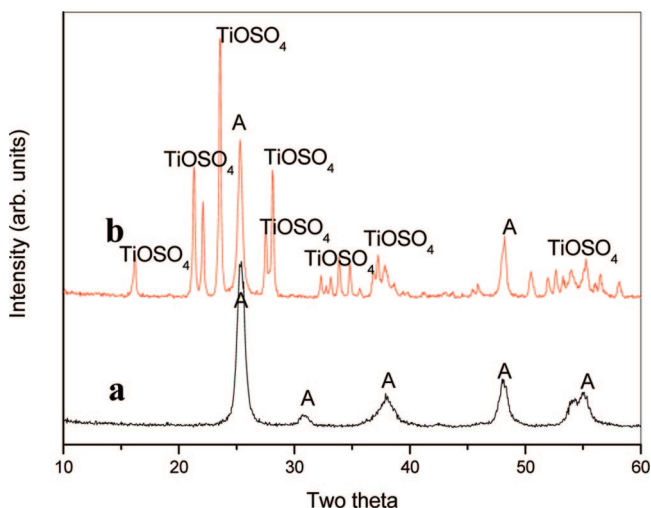


Figure 10. XRD of the samples calcined at 600 °C; (a) control, (b) TS4.

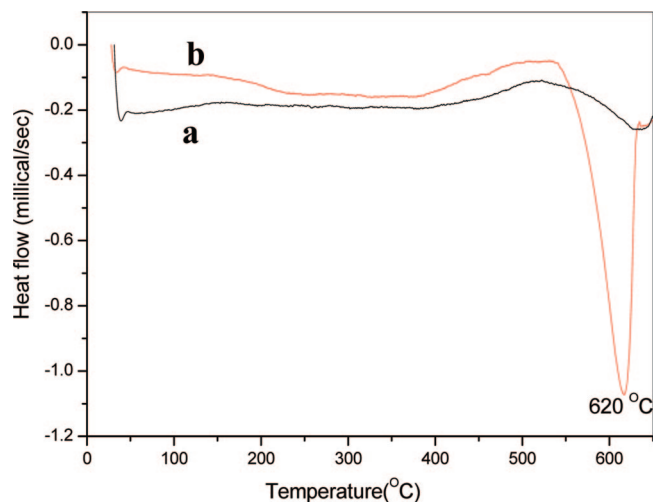


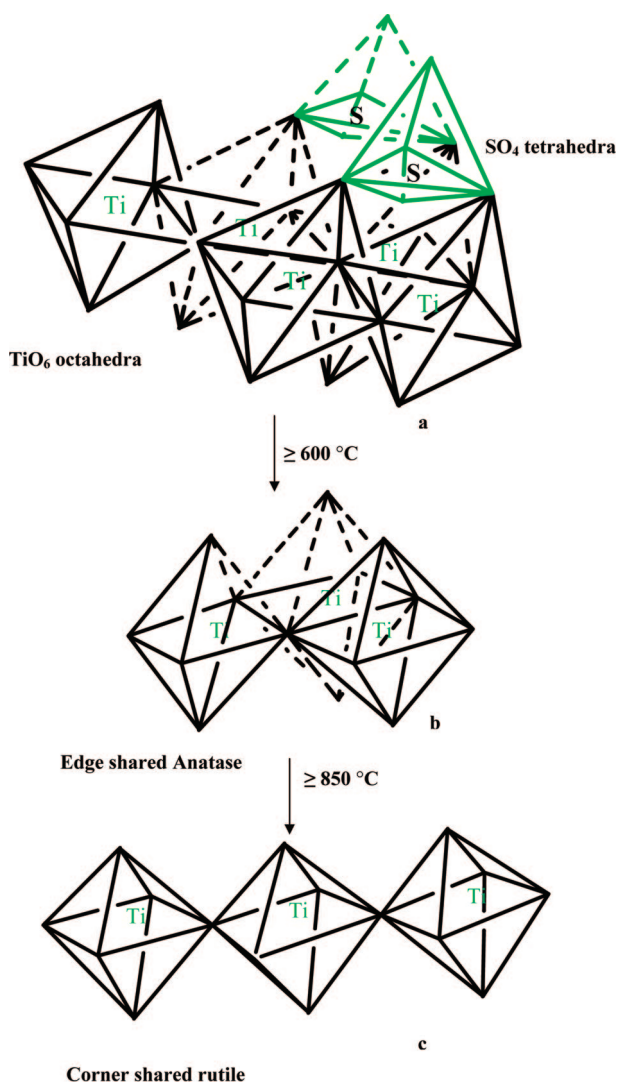
Figure 11. DSC curve of (a) the control and (b) TS4.

380 at 850 °C. This suggests that the anatase phase is stabilized as
 381 a result of sulfur doping due to the decrease in crystallite size.

382 It has been reported that sulfuric acid pretreatment on TiO₂
 383 particles provided 90% anatase at 700 °C but was completely
 384 transformed to rutile phase at 800 °C.^{18,19} In the present
 385 investigation, it appears that the S modification of TiO₂
 386 by sulfuric acid was effective in extending the anatase stability up
 387 to 900 °C. Although the lower mole percentage samples TS1
 388 and TS2 improved the anatase stability, gradual increments in

molar concentration of sulfuric acid showed that S modification
 of TiO₂ was most effective at four times the concentration of
 the titanium isopropoxide (TS4 sample). Studies of the phase
 transformation temperatures by XRD and Raman spectroscopy
 support this conclusion. During the calcination process, surface-
 adsorbed water, hydroxyl groups, and bridged OH groups
 attached to TiO₂ will be removed. This elimination causes the
 formation of an oxygen vacancy in the titania matrix.^{17,18} In
 these oxygen vacancy sites, the sulfur may be doped as an anion/
 cation, but it has been previously reported by Yu et al. that

389
 390
 391
 392
 393
 394
 395
 396
 397
 398

SCHEME 1: Schematic Representation of Decomposition of TiOSO₄ to Anatase and Its Transformation to Rutile (a: TiOSO₄; b: Anatase Titania; c: Rutile Titania)**TABLE 2: Crystallite Size of Anatase**

samples	Crystallite size of anatase (nm) ($\pm 5\%$)			
	700 °C	800 °C	850 °C	900 °C
control	17.7	^a	^a	^a
TS4	7.09	12.9	15.7	23.6

^a Anatase phase is transformed to rutile.

anionic sulfur doping is difficult to achieve because the ionic radius of the S²⁻ (1.7 Å) ion is larger than that of O²⁻ (1.22 Å).²¹ The bond strength of the Ti–S bond (418.0 kJ/mol) is less than the already existing Ti–O bond (672.4 kJ/mol).³⁰ Therefore, the substitution of Ti⁴⁺ by S⁶⁺ is chemically more favorable than the replacement of O²⁻ by S²⁻. In this study, the presence of S⁶⁺ ions (the oxidation state of sulfur in sulfuric acid is +6) in the titania lattice was confirmed by XPS measurement, which showed a peak at 168.4 eV (Figure 5).

4.2. Photocatalysis. Nanocrystalline titania exhibits photocatalytic activity in the presence of UV light, and it can decompose organic pollutants. This activity depends upon several factors, such as the rate of electron–hole recombination, the number of electrons created, the phase composition (anatase or rutile), the surface area, the crystallinity, as well as the crystallite size of the TiO₂ and the adsorption properties of the

dyes on the surface of the TiO₂ used.²⁹ The sulfur-modified sample exhibited higher photocatalytic activity than the control sample prepared under identical conditions. The photocatalytic activity of the control sample decreased with increased calcination temperature, whereas the sulfur-modified sample showed improvement in photocatalytic activity as the calcination temperature increased up to 850 °C (Supporting Information 1 and 2). It has been reported that the adsorption affinity of the anatase phase for the organic compound is higher than that of rutile, and anatase exhibits lower rates of recombination in comparison with those for rutile due to its 10-fold greater rate of electron trapping.⁴⁵ In this particular study, the anatase phase stability of the nanocrystalline TiO₂ powders at high calcination temperatures due to the sulfur doping is the main reason for the high photocatalytic activity. Sulfur doping leads to three main improvements in the modified sample. First, sulfur doping significantly increased the surface area of the high-temperature stable anatase titania (Table 1), which leads to the improved adsorption and thereby higher concentration of the reactant rhodamine dye molecules near the active centers of titania. Second it significantly changed the band gap of high-temperature stable anatase titania (Supporting Information 3 and 4). Finally, it significantly reduced the crystallite size of the high-temperature stable anatase titania compared to that of the control samples (Table 2). Normally the surface of the TiO₂ is positively charged in acidic media and negatively charged in basic media.^{46,47} Thus, here, the rhodamine 6G dye tends to adsorb on the surface of the TiO₂ by the negatively charged carbonyl group of the dye. Both UV and visible light irradiation show a gradual decrease in absorption of the dye without any blue shift in absorption maxima (Figures 8 and 9). It has been reported that the blue shift in the absorption maxima represents the dye degradation pathway via the elimination of the diethyl group.^{46,48} Therefore, it has been possible to conclude here in our study that the active radical species (hydroxyl and super oxide radicals) generated during UV and visible light illumination attack the ring structure (chromophore) to induce a cleavage rather than attacking the diethyl amino group (auxochrome) to direct the complete degradation of the dye. Also, it should be noted that there are no extra peaks appearing in UV–visible spectra (Figures 8 and 9), which leads to the conclusion that the dye is not photobleached during the photocatalytic reaction.

The photocatalytic activity of the TS4 samples increased with an increase in calcination temperature (Supporting Information 1 and 2), and it decreased after 850 °C. The reason for the highest activity of the TS4 sample calcined at 850 °C can be explained by the critical crystallite size limit of the photocatalytic activity. It is well-known that the photocatalytic activity of nanocrystalline titania is strongly dependent on its crystallite size.^{44,49,50} The reported critical crystallite size limit of TiO₂ for better photocatalytic activity of nanocrystalline titania is ~ 15 nm. Above or below this value, the photocatalytic activity decreases.^{41,42} For a better photocatalytic performance, the rate of the surface charge carrier recombination process should be minimum, but the interfacial charge-transfer process should be maximum.⁴⁴ As the nanocrystalline size decreases, the number of active surface sites which enhance the rate of the interfacial charge-transfer process increases; hence, the photocatalytic activity also increases. However, after reaching a critical size (~ 15 nm), the surface charge recombination dominates; hence, it reduces the photocatalytic activity. In our case, the sulfur-modified sample reached this limit at 850 °C, which shows the highest activity among the various TS4 samples calcined at different temperatures.

5. Conclusions

High-temperature stable anatase (up to 20% weight fraction) titania, existing up to 900 °C, has been successfully prepared by chemically modifying the precursor with sulfuric acid. This method eliminates the formation of various secondary impurity phases such as metal titanates and/or metal oxides at high temperatures, which can lead to the reduction of the photocatalytic activity and phase stability of anatase titania. Sulfur doping in high-temperature stabilized anatase titania was easily achieved by the decomposition of TiOSO₄ formed by the initial reaction between titanium isopropoxide and sulfuric acid. The high-temperature stability of anatase titania and sulfur doping was investigated by different characterization techniques such as XRD, Raman spectroscopy, DSC, XPS, and BET surface area analysis. All of the sulfur-modified samples showed significantly higher photocatalytic activity compared to the control titania. The enhanced efficiency of the sulfur-modified titania photocatalyst is reflected in kinetic analysis. The pseudo-first-order rates for the oxidation of rhodamine dye by the sulfur-modified sample calcined at different temperature (700, 800, 850, and 900 °C) are significantly higher than those for the corresponding control samples. The TS4 composition calcined at 850 °C showed the visible light photocatalytic activity, and it decolorized the rhodamine 6G dye within 35 min (rate constant 0.069 min⁻¹), whereas the control sample prepared under identical conditions decolorized the dye after 3.5 h (rate constant 0.007 min⁻¹).

Acknowledgment. The authors would like to thank Enterprise Ireland for financial support. One of the authors P. Periyat acknowledges the R&D Strand I Award 2005 from DIT. The authors wish to thank Dr. Hugh Hayden and Dr. Anthony Betts for their valuable comments.

Supporting Information Available: Rate constant and photocatalytic activity data and spectra and diffuse reflectance spectra. This material is available free of charge via the Internet at <http://pubs.acs.org>.

References and Notes

- (1) (a) Kamat, P. V. *J. Phys. Chem. C* **2007**, *111*, 2834. (b) Parkin, I. P.; Palgrave, R. G. *J. Mater. Chem.* **2005**, *15*, 1689.
- (2) Pillai, S. C.; Periyat, P.; George, R.; McCormack, D. E.; Seery, M. K.; Hayden, H.; Colreavy, J.; Corr, D.; Hinder, S. J. *J. Phys. Chem. C* **2007**, *111*, 1605.
- (3) (a) Chen, X.; Mao, S. S. *Chem. Rev.* **2007**, *107*, 2891. (b) Yamagishi, M.; Kuriki, S.; Song, P. K.; Shigesato, Y. *Thin Solid Films* **2003**, *442*, 227.
- (4) Bach, U.; Corr, D.; Lupo, D.; Pichot, F.; Ryan, M. *Adv. Mater.* **2002**, *14*, 845.
- (5) (a) Wang, X.; Yu, J. C.; Ho, C.; Hou, Y.; Fu, X. *Langmuir* **2005**, *21*, 2552. (b) Gratzel, M. *Nature* **2001**, *414*, 338.
- (6) (a) Hoffmann, M. R.; Martin, S. T.; Choi, W.; Bahnemann, D. W. *Chem. Rev.* **1995**, *95*, 69. (b) Yang, S. W.; Gao, L. *J. Am. Ceram. Soc.* **2005**, *88*, 968.
- (7) (a) Wang, H.; Miao, J. J.; Zhu, J. M.; Ma, H. M.; Zhu, J. J.; Chen, H. Y. *Langmuir* **2004**, *20*, 11738. (b) Baiju, K. V.; Sibin, C. P.; Rajesh, K.; Pillai, P. K.; Mukundan, P.; Warriar, K. G. K.; Wunderlich, W. *Mater. Chem. Phys.* **2005**, *90*, 123.
- (8) Baiju, K. V.; Periyat, P.; Pillai, P. K.; Mukundan, P.; Warriar, K. G. K.; Wunderlich, W. *Mater. Lett.* **2007**, *61*, 1751.
- (9) Machida, M.; Norimoto, W. K.; Kimura, T. *J. Am. Ceram. Soc.* **2005**, *88*, 95.
- (10) Periyat, P.; Baiju, K. V.; Mukundan, P.; Pillai, P. K.; Warriar, K. G. K. *J. Sol-Gel Sci. Technol.* **2007**, *43*, 299.
- (11) Ranjit, K. T.; Willner, I.; Bossmann, S. H.; Braun, A. M. *Environ. Sci. Technol.* **2001**, *35*, 154.

- (12) Sibin, C. P.; Kumar, S. R.; Mukundan, P.; Warriar, K. G. K. *Chem. Mater.* **2002**, *14*, 2876.
- (13) Kumar, K. N. P.; Kiezer, K.; Burggraaf, A. *J. Mater. Chem.* **1993**, *3*, 141.
- (14) Seery, M. K.; George, R.; Floris, P.; Pillai, S. C. *J. Photochem. Photobiol., A* **2007**, *189*, 258.
- (15) (a) Yu, J. C.; Ho, W.; Yu, J.; Hark, S. K.; Iu, K. *Langmuir* **2003**, *19*, 3889. (b) Suresh, C.; Biju, V.; Mukundan, P.; Warriar, K. G. K. *Polyhedron* **1998**, *17*, 3131.
- (16) Padmanabhan, S. C.; Pillai, S. C.; Colreavy, J.; Balakrishnan, S.; McCormack, D. E.; Perova, T. S.; Gun'ko, Y.; Hinder, S. J.; Kelly, J. M. *Chem. Mater.* **2007**, *19*, 4474.
- (17) Colon, G.; Hidalgo, M. C.; Munuera, G.; Ferino, I.; Cutrufello, M. G.; Navio, J. A. *Appl. Catal., B* **2006**, *67*, 41.
- (18) Colon, G.; Hidalgo, M. C.; Munuera, G.; Ferino, I.; Cutrufello, M. G.; Navio, J. A. *Appl. Catal., B* **2006**, *63*, 45.
- (19) Colon, G.; Espana, J. M. S.; Hidalgo, M. C.; Navio, J. A. *J. Photochem. Photobiol., A* **2006**, *179*, 20.
- (20) Ho, W.; Yu, J. C.; Lee, S. *J. Solid State Chem.* **2006**, *179*, 1171.
- (21) Yu, J. C.; Ho, W.; Yu, J.; Yip, H.; Wong, P. K.; Zhao, J. *Environ. Sci. Technol.* **2005**, *39*, 1175.
- (22) (a) Umebayashi, T.; Yamaki, T.; Itoh, H.; Asai, K. *Appl. Phys. Lett.* **2002**, *81*, 454. (b) Umebayashi, T.; Yamaki, T.; Tanala, S.; Asai, K. *Chem. Lett.* **2003**, *32*, 330. (c) Umebayashi, T.; Yamaki, T.; Yamamoto, S.; Miyashita, A.; Tanala, S.; Sumita, T.; Asai, K. *J. Appl. Phys.* **2003**, *93*, 5156.
- (23) (a) Ohno, T.; Mitsui, T.; Matsumura, M. *Chem. Lett.* **2003**, *32*, 364. (b) Ohno, T.; Akiyoshi, M.; Umebayashi, T.; Asai, K.; Mitsui, T.; Matsumura, M. *Appl. Catal., A* **2004**, *265*, 115.
- (24) Kuznetsov, V. N.; Serpone, N. *J. Phys. Chem. C* **2007**, *111*, 15277.
- (25) Serpone, N. *J. Phys. Chem. B* **2006**, *110*, 24287.
- (26) (a) Tachikawa, T.; Tojo, S.; Kawai, K.; Endo, M.; Fujitsuka, M.; Ohno, T.; Nishijima, K.; Miyamoto, Z.; Majima, T. *J. Phys. Chem. B* **2004**, *108*, 19299. (b) Bacsa, R.; Kiwi, J.; Ohno, T.; Albers, P.; Nadochenko, V. *J. Phys. Chem. B* **2005**, *109*, 5994.
- (27) Bokhimi, X.; Morales, A.; Novaro, O. *Chem. Mater.* **1997**, *9*, 2616.
- (28) Jung, H. S.; Shin, H.; Kim, J. R.; Kim, J. Y.; Hong, K. S. *Langmuir* **2004**, *20*, 11732.
- (29) Chen, X.; Lou, Y.; Samia, A. N. S.; Burda, C.; Gole, J. L. *Adv. Funct. Mater.* **2005**, *15*, 41.
- (30) Lide, D. R. *CRC Handbook of Physics and Chemistry*, 84th ed.; CRC: Boca Raton, FL, 2003.
- (31) Schubert, U. *J. Mater. Chem.* **2005**, *15*, 3701.
- (32) Schuth, F. *Chem. Mater.* **2001**, *13*, 3184.
- (33) Bringer, C. J.; Scherer, G. W. *Sol-Gel Science*; Academic Press: New York, 1990.
- (34) Choi, S. Y.; Mamak, M.; Coombs, N.; Chopra, N.; Ozin, G. A. *Adv. Funct. Mater.* **2004**, *14*, 335.
- (35) Pillai, S. C.; Boland, S. W.; Haile, S. M. *J. Am. Ceram. Soc.* **2004**, *87*, 388.
- (36) Boland, S. W.; Pillai, S. C.; Yang, W. D.; Haile, S. M. *J. Mater. Res.* **2004**, *19*, 1492.
- (37) Gopal, M.; Chan, W. J. M.; De Jonghe, L. C. *J. Mater. Sci.* **1997**, *32*, 6001.
- (38) Livage, J.; Henry, M.; Sanchez, C. *Prog. Solid State Chem.* **1998**, *18*, 259.
- (39) Gatehouse, B. M.; Platts, S. N.; Williams, T. B. *Acta Crystallogr.* **1993**, *49*, 428.
- (40) Wang, H.; Lewis, J. P. *J. Phys.: Condens. Matter* **2006**, *18*, 421.
- (41) Asahi, R.; Morikawa, T.; Ohwaki, K.; Aoki, T.; Taga, Y. *Science* **2001**, *293*, 269.
- (42) Zhang, H.; Banfield, J. F. *J. Mater. Chem.* **1998**, *8*, 2073.
- (43) Gribb, A. A.; Banfield, J. F. *Am. Mineral.* **1997**, *82*, 717.
- (44) Baiju, K. V.; Shukla, S.; Sandhya, K. S.; James, J.; Warriar, K. G. K. *J. Phys. Chem. C* **2007**, *111*, 7612.
- (45) Hurum, D. C.; Agrios, A. G.; Gray, K. A. *J. Phys. Chem. B* **2003**, *107*, 10871.
- (46) Chen, F.; Zhao, J.; Hidaka, H. *Int. J. Photoenergy* **2003**, *5*, 209.
- (47) Zhao, J.; Hidaka, H.; Takamura, A.; Pelizzetti, E.; Serpone, N. *Langmuir* **1993**, *9*, 1646.
- (48) Wilhelm, P.; Stephan, D. *J. Photochem. Photobiol., A* **2007**, *185*, 19.
- (49) Zhang, Z.; Wang, C. C.; Zakaria, R.; Ying, J. Y. *J. Phys. Chem. B* **1998**, *102*, 10871.
- (50) Inagaki, M.; Imai, T.; Yoshikawa, T.; Tryba, B. *Appl. Catal., B* **2004**, *51*, 247.